Separation Science and Technology
Publication details, including instructions for authors and subscription information:
http://www.informaworld.com/smpp/title~content=t713708471

Theory of Adsorption by Activated Carbon. II. Continuous Flow Columns

David J. Wilson[a]
[a] DEPARTMENTS OF CHEMISTRY AND ENVIRONMENTAL AND WATER RESOURCES ENGINEERING, VANDERBILT UNIVERSITY, NASHVILLE, TENNESSEE

To cite this Article Wilson, David J.(1979) 'Theory of Adsorption by Activated Carbon. II. Continuous Flow Columns', Separation Science and Technology, 14: 5, 415 — 430
To link to this Article: DOI: 10.1080/01496397908058094
URL: http://dx.doi.org/10.1080/01496397908058094

SEPARATION SCIENCE AND TECHNOLOGY, 14(5), pp. 415–430, 1979

Theory of Adsorption by Activated Carbon. II. Continuous Flow Columns

DAVID J. WILSON

DEPARTMENTS OF CHEMISTRY
AND ENVIRONMENTAL AND WATER RESOURCES ENGINEERING
VANDERBILT UNIVERSITY
NASHVILLE, TENNESSEE 37235

Abstract

A lumped parameter model for solute adsorption by activated carbon is used to model the operation of continuous flow activated carbon columns. A Langmuir adsorption isotherm is used, and the kinetics leading to the Langmuir isotherm are included in the continuity and mass balance equations representing the system. Two different approaches for the numerical integration of these equations are employed and compared. The effects of system parameters on column performance are explored.

INTRODUCTION

The role of activated carbon as a reasonably priced, regenerable adsorbent for trace organics in water is unique and well established (*1*). Common practice is to use the carbon in packed or expanded columns operated in a continuous flow mode. On near-saturation of the carbon, as evidenced by breakthrough of solute, the column is removed and regenerated.

Such adsorption columns were modeled many years ago by Thomas (*2, 3*) who assumed a constant flow rate, second-order kinetics, and no axial dispersion. He used the method of Riemann to obtain solutions in terms of the modified Bessel function I_0 and integrals involving I_0. Hiester and Vermeulen (*4*) also pursued this approach, and did not consider axial dispersion. Masamune and Smith (*5*) expressed the solutions to the problem in terms of integrals; in a later paper (*6*) they assumed a linear

isotherm and no axial dispersion, then solved the equations by use of double Laplace transforms. Keinath and Weber (*7*) neglected axial diffusion and obtained solutions to the equations in terms of exponentials and error functions. Keinath (*8*) has written computer programs to integrate the differential equations numerically, and exhibited the dependence of the breakthrough curves on the parameters of the model; he does not include axial dispersion in his model. Weber and his co-workers (*9–12*) have contributed extensively to the modeling of activated carbon columns, particularly with regard to biological processes going on in the columns.

These columns do not operate in a steady-state mode unless provision is made for countercurrent flow of the activated carbon, so it is necessary to examine the time-dependent continuity and mass balance equations which describe the system. In a continuous flow column, several processes are occurring simultaneously: bulk flow of free liquid along the length of the column, axial dispersion of free liquid along the length of the column, diffusion of solute in the free liquid to the mouths of the pores in the activated carbon, diffusion of solute into the trapped liquid within the pores, and adsorption and desorption of solute on the active sites on the surfaces of the pores. Unfortunately, even if we assume that diffusion of solute in the free liquid to the mouths of the pores is rapid, models including the remaining steps lead one to second-order nonlinear differential equations in three independent variables (time, distance down the column, and distance into the pores). The numerical integration of these equations requires such large amounts of computer time in realistic cases as to make this approach out of the question for practical design work.

We recently examined a rather realistic model for diffusion of solute from a large pool of liquid into a pore, followed by reversible chemisorption on the walls of the pore (*13*). Langmuir adsorption was assumed. The results of computations carried out with this model were compared with results obtained from a much simpler lumped parameter-type model for pore diffusion and chemisorption. We found that it was an easy matter to assign an effective pore diffusion parameter to the lumped parameter model, which made its results almost identical to those of the more elaborate and realistic model.

This is the basis for our use here of the lumped parameter model for pore diffusion and chemisorption in the construction of equations simulating the operation of continuous flow columns. We then compare two procedures for the numerical integration of these equations: (a) a standard predictor-corrector method described by Kelly (*14*) and used by us previously (*13*), and (b) a linearization method which permits the use of substantially larger time intervals in the numerical integration.

ANALYSIS

We first briefly examine the equations realistically modeling activated carbon column operation. We let

$c_l(y, t)$ = concentration of solute in the free liquid a distance y from the top of the column at time t

$c_p(x, y, t)$ = concentration of solute in the pore liquid a distance x from the mouth of the pore, located a distance y from the top of the column at time t

$\Gamma(x, y, t)$ = surface concentration of solute at (x, y, t)

Q = volumetric flow rate through column

v_l = volume of free (flowing) liquid per unit length of column

v_p = volume of liquid fixed in the pores of the carbon per unit length of column

s_p = surface area of pores per unit length of column

D_l = axial dispersion constant of solute in the flowing liquid

D_p = diffusion constant of solute in the pore liquid

Γ_{max} = maximum possible surface concentration of solute on the activated carbon

A_p = cross-sectional area of the pores per unit length of column

b = concentration of solute at which the equilibrium surface concentration of solute is $\Gamma_{max}/2$

k = rate constant for surface adsorption, assumed first order in c_p and in $\Gamma_{max} - \Gamma$

The equations representing flow of fluid through the column, axial dispersion, diffusion of solute into the pores, and surface chemisorption of solute are

$$\frac{\partial c_l}{\partial t}(y, t) = \frac{Q}{v_l}\frac{\partial c_l}{\partial y}(y, t) + \frac{D_l}{v_l}\frac{\partial^2 c_l}{\partial y^2}(y, t) + \frac{D_p A_p}{v_l}\frac{\partial c_p}{\partial x}(0, y, t) \qquad (1)$$

$$\frac{\partial c_p}{\partial t}(x, y, t) = \frac{D_p}{v_p}\frac{\partial^2 c_p}{\partial x^2}(x, y, t) - \frac{k s_p}{v_p}[c_p(x, y, t)\Gamma_{max} - c_p(x, y, t)\Gamma(x, y, t) - b\Gamma(x, y, t)], \qquad (2)$$

$$c_p(0, y, t) = c_l(y, t)$$

$$\frac{\partial c_p}{\partial x}(y, t) = 0, \; l = \text{pore length}$$

$$\frac{\partial \Gamma}{\partial t}(x, y, t) = k[c_p(x, y, t)\Gamma_{max} - c_p(x, y, t)\Gamma(x, y, t) - b\Gamma(x, y, t)] \quad (3)$$

These equations are nonlinear, so they must be integrated numerically. The diffusion and chemisorption processes within the individual pores dictate the use of a time increment of less than a tenth of a second, while the duration of a column run may be many hours. If one partitions the column into 20 horizontal slabs and similarly partitions the pores in each slab into 20 volume elements (rather coarse partitionings), we have some 820 simultaneous differential equations to be integrated forward over roughly 1.5 million time increments, assuming $\Delta t \cong 0.1$ sec and a 40-hr column run. Such large amounts of computation make this approach impractical for use as a design tool.

We therefore construct a set of equations based upon the lumped parameter model to simulate column operation. The model is illustrated in Fig. 1, and the previous notation is modified as follows:

$c_l(i, t)$ = concentration of solute in the free liquid in the i-th slab into which the column is partitioned
$c_p(i, t)$ = concentration of solute in the pore liquid in the i-th slab
$\Gamma(i, t)$ = surface concentration of solute in the pores of the i-th slab

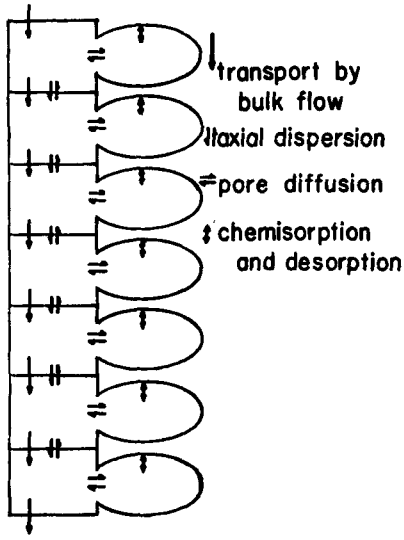

FIG. 1. The model used to simulate column operation.

v_l = volume of free liquid in one slab
v_p = volume of liquid in the pores of one slab
s_p = surface area of the pores in one slab
D_l = effective axial dispersion constant
D_p = effective pore diffusion constant

Inclusion of axial dispersion in this model leads us to second-order nonlinear differential equations which cannot be solved by the method employed by Thomas and others (*2–4*). We therefore approximate the partial differential equations by means of a finite difference mesh system. The differential equations representing this model are

$$v_l \frac{\partial c_l}{\partial t}(j, t) = Q[c_l(j-1) - c_l(j)] + D_l[c_l(j-1) - 2c_l(j) + c_l(j+1)] + D_p[c_p(j) - c_l(j)] \tag{4}$$

$$v_p \frac{\partial c_p}{\partial t}(j, t) = D_p[c_l(j) - c_p(j)] - s_p \frac{\partial \Gamma}{\partial t}(j) \tag{5}$$

$$\frac{\partial \Gamma}{\partial}(j, t) = k[c_p(j)\Gamma_{max} - c_p(j)\Gamma(j) - b\Gamma(j)] \tag{6}$$

Substitution of Eq. (6) into Eq. (5) yields

$$v_p \frac{\partial c_p}{\partial t}(j, t) = D_p[c_l(j) - c_p(j)] - s_p k[c_p(j)\Gamma_{max} - c_p(j)\Gamma(j) - b\Gamma(j)] \tag{7}$$

Our first method for the numerical integration of Eqs. (4), (6), and (7) is a predictor-corrector method which we have used extensively previously and found to be accurate and stable. The algorithm is as follows:

predictor starter

$$y_i^*(\Delta t) = y_i(0) + \Delta t \frac{dy_i}{dt}(0) \tag{8}$$

predictor general

$$y_i^*(t + \Delta t) = y_i(t - \Delta t) + 2\Delta t \frac{dy_i}{dt}(t) \tag{9}$$

corrector

$$y_i(t + \Delta t) = y_i(t) + \frac{\Delta t}{2}\left[\frac{dy_i}{dt}(t) + \frac{dy_i^*}{dt}(t + \Delta t)\right] \tag{10}$$

As we shall see under "Results," this procedure works rather well. It does, however, lead to disastrous instabilities if the size of Δt is sufficiently large that the pore diffusion, axial dispersion, or chemisorption terms in Eqs. (4), (6), and (7) lead to negative concentrations because of the assumption in the predictor formula that these terms, as they appear in Eq. (9), are linear in Δt. A similar problem arises with the terms involving Q (free fluid flow) in Eq. (6), but here one can evade the problem by choosing the slab thickness Δx larger; one must have $Q\Delta t < v_l$.

For reasons of economy in the numerical integration of this system of equations, one would like to be able to use larger values of Δt than the predictor-corrector method permits. We develop a method of solution in which the dependent variables vary in an exponential way with time over the interval $(t, t + \Delta t)$ rather than in a linear way.

We focus our attention on the equations in the time interval $(t, t + \Delta t)$ and let $t + \tau$ be the time variable; τ increases from 0 to Δt continuously. We let

$$c_l(j, t + \tau) = c_l(j, t) + \psi_l(j, \tau) \tag{11}$$

$$c_p(j, t + \tau) = c_p(j, t) + \psi_p(j, \tau) \tag{12}$$

$$\Gamma(j, t + \tau) = \Gamma(j, t) + \gamma(j, \tau) \tag{13}$$

Insertion of these expressions into Eqs. (4), (6), and (7), and neglect of terms quadratic in ψ_l, ψ_p, and γ, lead to the following system of linear differential equations with constant (independent of τ) coefficients for the ψ_l, ψ_p, and γ:

$$\begin{aligned}\frac{d\psi_l}{d\tau}(j, \tau) = \frac{1}{v_l}\{&Q[c_l(j-1, t) - c_l(j, t)] \\ &+ D_l[c_l(j-1, t) - 2c_l(j, t) + c_l(j+1, t)] \\ &+ D_p[c_p(j, t) - c_l(j, t)] + Q[\psi_l(j-1, \tau) - \psi_l(j, \tau)] \\ &+ D_l[\psi_l(j-1, \tau) - 2\psi_l(j, \tau) + \psi_l(j+1, \tau)] \\ &+ D_p[\psi_p(j, \tau) - \psi_l(j, \tau)]\}\end{aligned} \tag{14}$$

$$\begin{aligned}\frac{d\psi_p}{d\tau}(j, \tau) = \frac{1}{v_p}\{&D_p[c_l(j, t) - c_p(j, t)] - s_p k[c_p(j, t)\Gamma(j, t) - b\Gamma(j, t)] \\ &+ D_p[\psi_l(j, \tau) - \psi_p(j, \tau)] - s_p k[\psi_p(j, \tau)\Gamma_{\max} \\ &- c_p(j, t)\gamma(j, \tau) - \Gamma(j, t)\psi_p(j, \tau) - b\gamma(j, \tau)]\}\end{aligned} \tag{15}$$

$$\frac{d\gamma}{d\tau}(j,\tau) = k[c_p(j,t)\Gamma_{\max} - c_p(j,t)\Gamma(j,t) - b\Gamma(j,t)] + k[\psi_p(j,\tau)\Gamma_{\max} - c_p(j,t)\gamma(j,\tau) - \Gamma(j,t)\psi_p(j,\tau) - b\gamma(j,\tau)] \tag{16}$$

We must modify Eq. (4) for $j = 1$ and N, the top and bottom of the column; these boundary equations are

$$v_l\frac{\partial c_l}{\partial t}(1,t) = Q[c_l^0(t) - c_l(1,t)] + D_l[-c_l(1,t) + c_l(2,t)] + D_p[c_p(1,t) - c_l(1,t)] \tag{17}$$

and

$$v_l\frac{\partial c_l}{\partial t}(N,t) = Q[c_l(N-1,t) - c_l(n,t)] + D_l[c_l(N-1,t) - c_l(N,t)] + D_p[c_p(n,t) - c_l(N,t)] \tag{18}$$

where $C_l^0(t)$ = influent solute concentration.

When these equations are linearized, we obtain

$$\frac{d\psi_l}{d\tau}(1,\tau) = \frac{1}{v_l}\{Q[c_l^0(t) - c_l(1,t)] + D_l[-c_l(1,t) + c_l(2,t)] + D_p[c_p(1,t) - c_l(1,t)] + [-Q - D_l - D_p]\psi_l(1,\tau) + D_l\psi_l(2,\tau) + D_p\psi_p(1,\tau)\} \tag{19}$$

and

$$\frac{d\psi_l}{d\tau}(N,\tau) = \frac{1}{v_l}\{Q[c_l(N-1,t) - c_l(N,t)] + D_l[c_l(N-1,t) - c_l(N,t)] + D_p[c_p(N,t) - c_l(n,t)] + [Q + D_l]\psi_l(N-1,\tau) + [-Q - D_l - D_p]\psi_l(N,\tau) + D_p\psi_p(N,\tau)\} \tag{20}$$

We rewrite Eqs. (14), (15), (16), (19), and (20) in a much more compact matrix notation as

$$\frac{d}{d\tau}\begin{pmatrix}\psi_l(1,\tau)\\ \vdots \\ \gamma(N,\tau)\end{pmatrix} = \begin{pmatrix}F_1(t)\\ \vdots \\ F_{3N}(t)\end{pmatrix} + \mathbf{A}(t)\begin{pmatrix}\psi_l(1,\tau)\\ \vdots \\ \gamma(N,\tau)\end{pmatrix} \tag{21}$$

or still more compactly, as

$$dY/d\tau = \mathbf{F}_0(t) + \mathbf{A}(t)\mathbf{Y} \tag{22}$$

We employ as a trial solution the vector

$$\mathbf{Y} = \mathbf{C}_1 + \exp(\mathbf{A}\tau)\mathbf{C}_2 \tag{23}$$

and note that $Y(\tau = 0)$ must vanish; substitution in Eq. (22) establishes that

$$\mathbf{C}_1 = -\mathbf{A}^{-1}\mathbf{F}_0 \tag{24}$$

$$\mathbf{C}_2 = \mathbf{A}^{-1}\mathbf{F}_0 \tag{25}$$

so our solution is

$$\mathbf{Y}(\tau) = -\mathbf{A}^{-1}[\mathbf{I} - \exp(\mathbf{A}\tau)]\mathbf{F}_0 \qquad (\mathbf{I} = \text{identity matrix}) \tag{26}$$

The matrix exponential is defined by the usual power series; use of this expression in Eq. (26) permits us to avoid the indicated matrix inversion and yields

$$\mathbf{Y} = \tau\left(\mathbf{I} + \frac{\mathbf{A}\tau}{2!} + \frac{\mathbf{A}^2\tau^2}{3!} + \frac{\mathbf{A}^3\tau^3}{4!} + \cdots\right)F_0 \tag{27}$$

The power series is convergent for all finite τ and $\mathbf{A}$. We set $\tau = \Delta t$, calculate $\mathbf{Y}(\Delta t)$, recall that

$$\mathbf{Y}(\Delta t) = \begin{pmatrix} \psi_I(1, \Delta t) \\ \vdots \\ \gamma(N, \Delta t) \end{pmatrix} \tag{28}$$

and use Eqs. (11)–(13) to calculate the $c_I(j, t + \Delta t)$, $c_p(j, t + \Delta t)$, $\Gamma(j, t + \Delta t)$. These new values are then used to calculate $\mathbf{F}_0(t + \Delta t)$ and $\mathbf{A}(t + \Delta t)$, and the process outlined above is repeated until integration of the differential equations over the desired time interval is complete.

In carrying out the numerical integrations by this method, we note that the bulk of the computer time is used in evaluating the matrix power series in Eq. (27). We observe that this power series can be rewritten:

$$I + \frac{\mathbf{A}\tau}{2!} + \frac{\mathbf{A}^2\tau^2}{3!} + \frac{\mathbf{A}^3\tau^3}{4!} + \cdots \ (n \text{ terms})$$

$$= \left(I + \frac{\mathbf{A}\tau}{2}\left(I + \frac{\mathbf{A}\tau}{3}\left(\cdots\left(I + \frac{\mathbf{A}\tau}{n-1}\left(I + \frac{\mathbf{A}\tau}{n}\right)\right)\cdots\right)\right)\right) \tag{29}$$

The matrix $\mathbf{A}$ is sparse—it has relatively few nonzero elements and these are distributed as follows:

$\mathbf{A} =$ 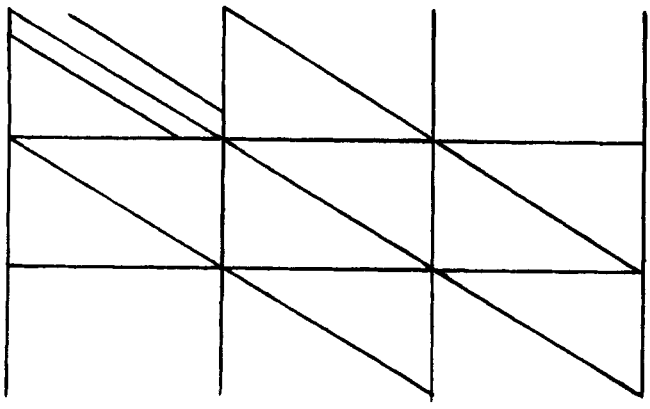 (30)

where each diagonal line indicates the presence of a single diagonal of nonzero matrix elements. Evidently in the ij-th element of the matrix product **AB**,

$$c_{ij} = \sum_k a_{ik} b_{kj} \tag{31}$$

there are only 2, 3, or 4 nonzero terms. Writing a special matrix multiplication subroutine to capitalize on this speeds this method up greatly.

RESULTS

All computations were carried out on an XDS Sigma 7 computer. The column was partitioned into 20 slabs unless noted otherwise. The calculation of a breakthrough curve by the first, predictor-corrector method, took 5 min of machine time. Figures 2–10 present results obtained by the method.

In Fig. 2 we see the effect of varying the adsorption rate constant k. The curve for $k = \infty$ was calculated using a program which assumed equilibrium between the concentration of solute in the pore liquid and the pore surface concentration of the solute. Increasing k results in a very marked improvement in the shape of the breakthrough curve; leakage through the column before saturation is drastically reduced. Almost exactly the same effect is observed when one increases the diffusion constant of the solute into the pores, as shown in Fig. 3. Figure 4 shows the effect of varying the pore diffusion constant D_p when k is infinite. It is difficult to see how one could experimentally distinguish between control

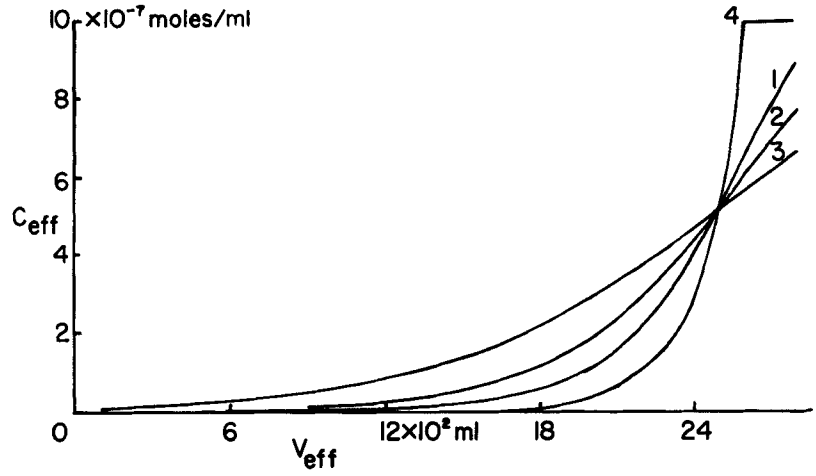

FIG. 2. Dependence of breakthrough curves (effluent concentration versus effluent volume) on adsorption rate constant k. $k = 2 \times 10^4$ (1), 10^4 (2), 5×10^3 (3), and ∞ (4) cm^3/mole sec; $Q = 2.0$ cm^3/sec; $D_l = 0.0$ cm^3/sec; $D_pA_p = 2.0$ cm^4/sec; $b = 10^{-8}$ mole/cm^3; $\Gamma_{max} = 3 \times 10^{-10}$ cm^2; $s_p = 4 \times 10^5$ cm^2; $v_p = 1.0$ cm^3; $v_l = 1.0$ cm^3; $c_0 = 10^{-6}$ mole/cm^3; $\Delta t = 0.1$ sec; $n = 20$.

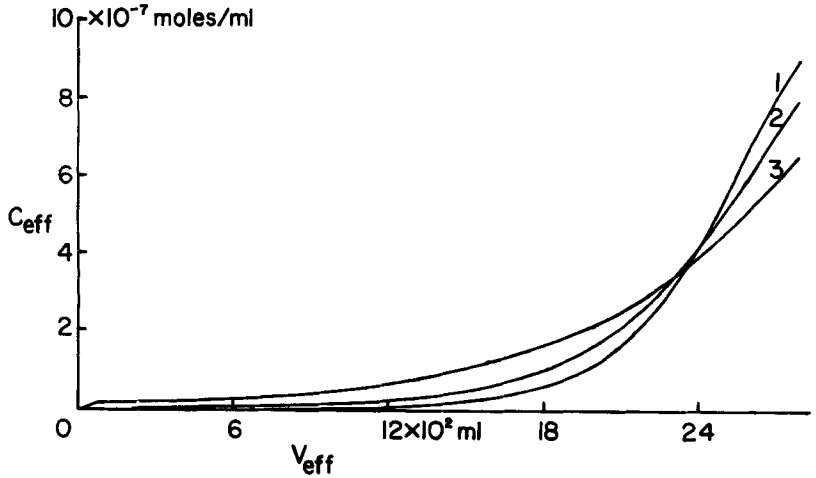

FIG. 3. Dependence of breakthrough curves on pore diffusion parameter D_pA_p. $D_pA_p = 2.0$ (1), 1.0 (2), and 0.5 (3) cm^4/sec; $k = 2 \times 10^4$ cm^3/mole sec. Other parameters as in Fig. 2.

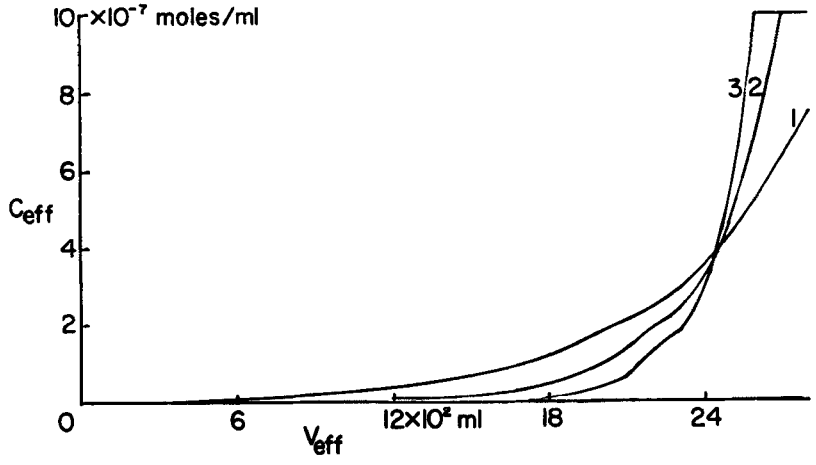

FIG. 4. Dependence of breakthrough curves on pore diffusion parameter D_pA_p. D_pA_p = 2.0 (1), 1.0 (2), and 0.5 (3) cm⁴/sec; $k = \infty$. Other parameters as in Fig. 2.

of breakthrough curve shape by adsorption rate constant k and control by pore diffusion constant D_p.

Figure 5 shows the effect of axial dispersion on column performance; as expected, increased axial dispersion results in greater leakage of solute through the column before saturation. We also found that increasing the axial dispersion constant above a certain point (D_l = 1.0 if Δt = 0.1 sec and Δx = 2.5 cm) results in the abrupt onset of catastrophic instabilities in the numerical integration. A run was made with D_l = 1.5, Δt = 0.05; the numerical integration proceeded satisfactorily for this run, indicating that the instability is a mathematical artifact and not an indication of instability in the underlying physical system. We found it surprising that the shapes of the breakthrough curves are so little affected by increasing the value of the axial dispersion constant.

One can also take account of increased axial dispersion by decreasing the number of slabs into which the column is partitioned; this avoids the instability problem which arises if D_l is made too large, and also reduces the amount of computer time required. As seen in Fig. 6, the magnitude of the effect is small and is indistinguishable from the results obtained by varying D_l. Our findings indicate that axial dispersion does not contribute significantly to the shapes of the breakthrough curves and is generally

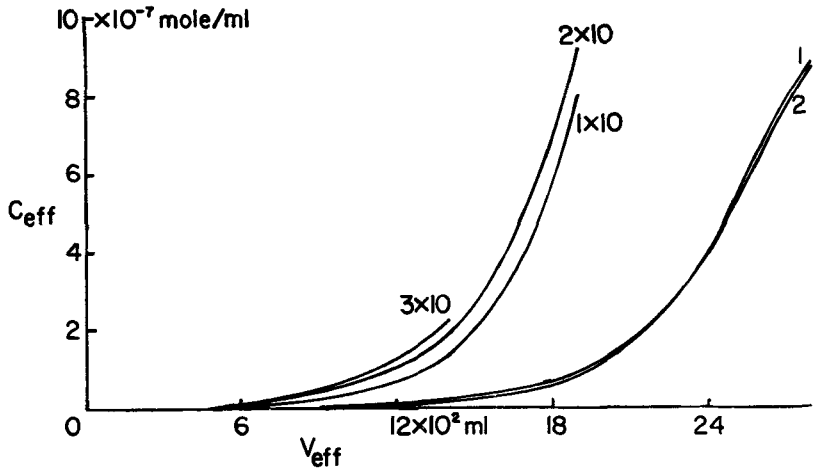

FIG. 5. Dependence of breakthrough curves on axial dispersion constant D_l. $D_l = 0.0$ (1), 0.9 (2), and 1.5 cm³/sec (3); $k = 2 \times 10^4$ cm³/mole sec. Other parameters as in Fig. 2.

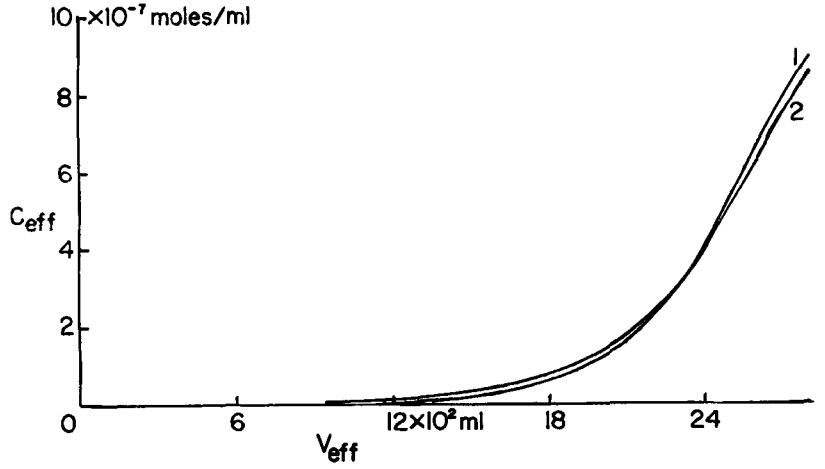

FIG. 6. Dependence of breakthrough curves on number of slabs n. $n = 20$, $D_p A_p = 2.0$ cm⁴/sec, $s_p = 4 \times 10^5$ cm², $v_p = 1.0$ cm³, and $v_l = 1.0$ cm³ for Run 1. $n = 10$, $D_p A_p = 4.0$ cm⁴/sec, $s_p = 8 \times 10^5$ cm², $v_p = 2.0$ cm³, and $v_l = 2.0$ cm³ for Run 2. $k = 2 \times 10^4$ cm³/mole sec; other parameters as in Fig. 2.

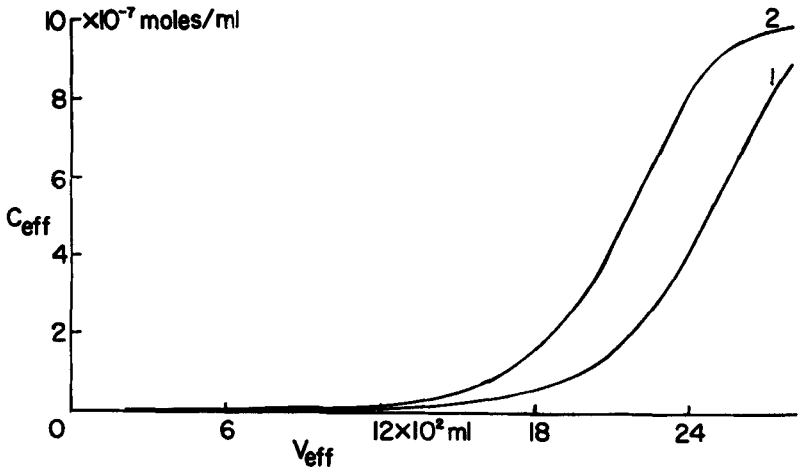

FIG. 7. Dependence of breakthrough curves on pore volume parameter v_p. v_p = 1.0 (1) and 0.5 (2) cm^3; $k = 2 \times 10^4$ cm^3/mole sec; other parameters as in Fig. 2.

best handled by the choice of the number of slabs into which the column is partitioned.

The effect of pore volume is seen in Fig. 7; the major contribution seems to be due simply to the solute storage capacity of the trapped liquid in the pores, with the curve corresponding to the larger pore volume being displaced to the right. The strength of the binding of solute to active sites in the pores is measured by the Langmuir parameter b, the solute concentration at half surface saturation; binding strength increases as b decreases. In Fig. 8 we see that, as expected, breakthrough occurs sooner the larger the value of b.

Increasing the volumetric flow rate through the column results in some deterioration of column performance, as illustrated in Fig. 9. Other computations, not shown here, indicate that the magnitude of this effect is strongly dependent on the values of k and D_p. Increased flow rates decrease somewhat the effect of increased axial dispersion constants, but the effect is small.

Figure 10 shows the effect of increasing solute concentration on the shapes of the breakthrough curves. The breakthrough front becomes substantially sharper as we go to higher solute concentrations.

Several runs were made using the second approach, outlined in Eqs. (11)–(30), and we found that the magnitude of Δt which could be used

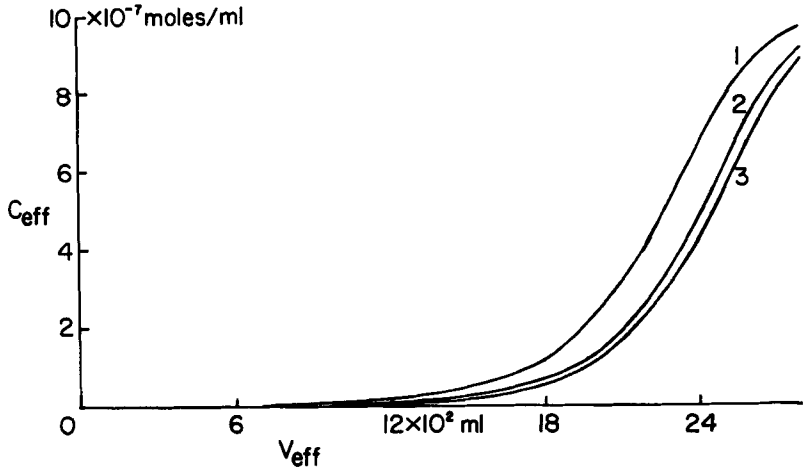

FIG. 8. Dependence of breakthrough curves on Langmuir parameter b. $b = 10^{-7}$ (1), 3×10^{-8} (2), and 10^{-8} mole/cm^3 (3); $k = 2 \times 10^4$ cm^3/mole sec; other parameters as in Fig. 2.

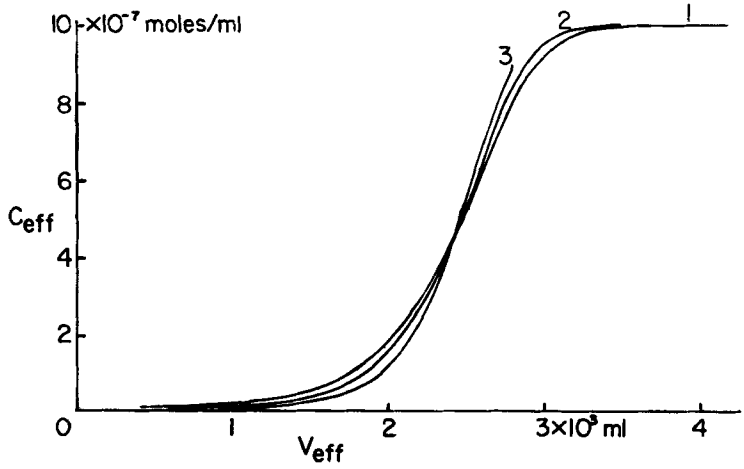

FIG. 9. Dependence of breakthrough curves on flow rate Q. $Q = 3.0$ (1), 2.5 (2), and 2.0 (1) cm^3/sec; $k = 2 \times 10^4$ cm^3/mole sec; other parameters as in Fig. 2.

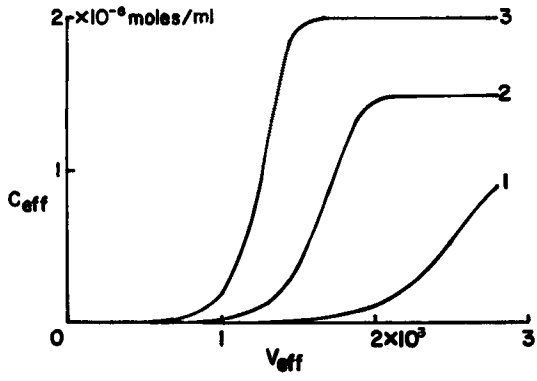

FIG. 10. Dependence of breakthrough curves on influent solute concentration c_0. c_0 = 1.0 (1), 1.5 (2), and 2.0 (3) $\times$ 10^{-6} mole/cm^3; $k = 2 \times 10^4$ cm^3/mole sec; other parameters as in Fig. 2.

without instability increased by a factor of about 5 above that which could be used with the predictor-corrector method. The breakthrough curves calculated by the two methods for a given run were identical to four places. Unfortunately, even with the larger value of Δt which could be used, the second approach was substantially slower than the predictor-corrector method. Even with the streamlining of the matrix multiplication procedure described above, the running time of the second method is of order n^2, where n is the number of slabs into which the column is divided. The predictor-corrector method, on the other hand, is of order n. Evidently the second method is likely to be competitive only for relatively small values of n.

CONCLUSIONS

In summary, we conclude that the effects of axial dispersion are rather slight and are best taken into account by adjustment of the number of slabs into which the column is partitioned. The effects of adsorption rate constant k and pore diffusion constant are large and essentially indistinguishable. The predictor-corrector method of integrating the differential equations gives results identical to a more elaborate approach and is generally substantially faster.

Acknowledgment

This work was supported by a grant from the National Science Foundation.

REFERENCES

1. *Process Design Manual for Activated Carbon Adsorption*, first revision, U.S. Environmental Protection Agency, Technology Transfer, October 1973.
2. H. C. Thomas, *J. Am. Chem. Soc.*, *66*, 1664 (1944).
3. H. C. Thomas, *Ann. N. Y. Acad. Sci.*, *49*, 161 (1948).
4. N. K. Hiester and T. Vermeulen, *Chem. Eng. Prog.*, *48*, 505 (1952).
5. S. Masamune and J. M. Smith, *Ind. Eng. Chem., Fundam.*, *3*, 179 (1964).
6. S. Masamune and J. M. Smith, *AIChE J.*, *11*, 34 (1965).
7. T. M. Keinath and W. J. Weber, Jr., *J. Water Pollut. Control Fed.*, *40*, 741 (1968).
8. T. M. Keinath, in T. M. Keinath and M. P. Wanielista (eds.), *Mathematical Modeling for Water Pollution Control Processes*, Ann Arbor Science Publishers, Ann Arbor, Michigan, 1975, Chap. 1.
9. W. J. Weber, Jr., *Physicochemical Processes for Water Quality Control*, Wiley-Interscience, New York, 1972, Chap. 5.
10. W. J. Weber, Jr., L. D. Friedman, and R. Bloom, Jr., "Biologically-Extended Physicochemical Treatment," in *Proceedings of the 6th Conference of the International Association for Water Pollution Research*, Pergamon Press, Oxford, 1973.
11. W. J. Weber, Jr., and W.-C. Ying, "Integrated Biological and Physicochemical Treatment for Reclamation of Wastewater," in *Proceedings of the International Conference on Advanced Treatment and Reclamation of Wastewater*, International Association for Water Pollution Research, Johannesburg, South Africa, June 1977.
12. W.-C. Ying, "Investigation and Modeling of Bio-Physicochemical Processes in Activated Carbon Columns," Ph.D. Dissertation, The University of Michigan, Ann Arbor, Michigan, 1978.
13. D. J. Wilson and A. N. Clarke, *Sep. Sci. Technol.*, *14*, 227–241 (1979).
14. L. G. Kelly, *Handbook of Numerical Methods and Applications*, Addison-Wesley, Reading, Massachusetts, 1967, p. 186.

Received by editor September 13, 1978